Flat dynamic model analysis of a delta-wing convertible aircraft

Monika Pasquali, Tudor-Bogdan Airimitoaie, Patrick Lanusse

Flat dynamic model analysis of a delta-wing convertible aircraft ⋆

Monika Pasquali * **Tudor-Bogdan Airimitoaie** *
Patrick Lanusse *

* *Univ. Bordeaux, CNRS, Bordeaux INP, IMS, 33405 Talence, France*
(e-mail: firstname.lastname@u-bordeaux.fr)

Abstract: This paper proposes the study of a tail-sitter, delta-wing, convertible aircraft that combines the advantages of vertical take-off and landing (VTOL) and fixed-wing aircraft. Control during the transition between VTOL and horizontal flight, as well as the design of fault detection and isolation (FDI) algorithms should be considered to ensure safe operation. The main contribution of the paper is in the analysis of the flatness property of the convertible aircraft. Flat systems have the property that their inputs and states can be written as functions of a set of variables called flat outputs and their derivatives. Thus, an inverse dynamic model can be obtained which can be used to design path planning, nonlinear feedforward control, and FDI algorithms. First, the analysis of flatness in the horizontal flight is presented. Then, it is shown that this first set of flat outputs is singular at hover flight. Fortunately, this is only an apparent singularity as a second set of flat outputs can be obtained, which defines a chart of the aircraft's dynamical model at hover and slow aerodynamic speed.

Keywords: Aerospace Control Systems, UAVs, convertible aircraft, autonomous vehicles, non-linear systems, algebraic/geometric methods

1. INTRODUCTION

Unmanned aerial vehicles (UAVs) made their initial appearance in the military as remote-control aircrafts, but nowadays are widely used also in civil applications. As Phung (2015) reports, UAVs were traditionally classified into: fixed-wing and vertical take-off landing (VTOL). Concerning fixed-wing UAVs, the flight is mainly based on the propellers' thrust to cancel the drag induced by the air movement and the aerodynamic lift on the wings to compensate for the weight of the vehicle. These vehicles are very efficient in the forward flight and they require runways for take-off and landing. VTOL UAVs, in contrast, have the ability to hover, but are not very efficient in forward flight. Increasingly popular are *convertible* aircrafts which combine the advantages of VTOL and fixed-wing aircrafts. From the first, they take their ease of maneuverability at slow speed, while from the second they inherit the energy efficiency in fast horizontal flight. As such, they are good candidates for many real-world applications (see WingtraOne (2023) and its fields of applications).

Among the possible diverse configurations for a convertible aircraft (Basset et al. (2014)), this paper is focused on the tilt-body aerial vehicles, which are increasingly popular in unmanned applications. Tilt-body convertible UAVs require the body of the aircraft to rotate during the transition flight and, additionally, wings and rotor hubs are rigidly attached to the aircraft body. Also, a special kind of tilt-body aircraft, which is considered here, is the so-called tail-sitter due to the ability to take-off and land on its tail (Kubo (2006)).

In this paper, first the nonlinear dynamic model of the delta-wing convertible aircraft is presented, which is largely built on previous work by Airimitoaie et al. (2019). The intent of the model is to provide a foundation for the paper's main contribution, namely the proof of the differential flatness property of the model, under given assumptions.

Flat systems have the property that their inputs and states can be written as functions of a set of variables called flat outputs and their derivatives (Lévine (2009)). Thus, an inverse dynamic model can be obtained which can be used to design path planning and nonlinear feedforward control (see Louembet et al. (2010); Formentin and Lovera (2011); Joos et al. (2019)), and FDI algorithms (Torres (2014)).

The differential flatness analysis of a tailsitter UAV proposed in this paper can be compared with the one from Tal and Karaman (2022); Tal et al. (2023), where the modelling approach using the ϕ-theory parametrisation from Lustosa (2017) is used. As in these papers, the aircraft representation for the flatness analysis is done based on Euler angles. It is well known that Euler angles can lose one degree of freedom when two axes of rotation align, phenomenon better known as Gimbal lock, which can occur in acrobatic flight maneuvers.

The solution proposed in the present paper is to introduce a second set of Euler angles, complementary to the first one in the sense that one can switch between them to avoid

⋆ This research was funded, in part, by l'Agence Nationale de la Recherche (ANR), project MICA ANR-16-CE22-0003.

Gimbal lock at all configurations in space. The flatness property is first analysed in the fast horizontal flight and a flat output is proposed. Then, analysis in hover flight shows that this initial set of flat outputs is singular in this case (see Kaminski et al. (2018) for a definition of intrinsic and apparent singularities of differentially flat systems). Fortunately, this singularity is only apparent as a second set of flat outputs can be found for hover and slow speeds.

This paper is organized as follows. Section 2 introduces the notations and conventions that will be used. The system is described in Section 3. In Section 4 the forces and moments acting on the aircraft are given and the nonlinear model, using the Newton-Euler formalism, is shown in Section 7. This model is used for the flatness analysis in horizontal flight, illustrated in Section 8.1, since it uses Euler angles for attitude description, which are not suitable to deal with the gimbal lock issue. Hence, for the vertical and hover flight modes, a modification of this model and its related flatness analysis is proposed in Section 8.2. Concluding remarks are given in Section 9.

2. NOTATIONS AND ASSUMPTIONS

Notations and assumptions similar to those in Airimitoaie et al. (2018) are used. They are recalled in this section for completeness. The trigonometric functions sin, cos, tan are abbreviated into c, s, t respectively, and in some of the following equations the dependence on time (t) is avoided to save space.

A constant gravity field is assumed, hence the Center of Mass (CoM) of the aircraft coincides with its Center of Gravity (CG). The earth is assumed flat and fixed.

The reference frames are indicated with upper-case calligraphic letters and the lower-case superscripts denote the projection frames, and are expressed with the right-hand rule.

The inertial-frame $\mathcal{I} = (O; x^i, y^i, z^i)$ has the origin O at the surface of the earth and the North-East-Down (NED) convention is used to define its axis x^i, y^i, z^i.

The vehicle-carried normal Earth $\mathcal{O} = (CG; x^o, y^o, z^o)$, has the origin at the CG of the aircraft and its axes are parallel to those of $\mathcal{I}$. The gravitational force vector is defined in this frame as $G^o = [0, 0, mg]^\intercal$.

The body-frame $\mathcal{B} = (CG; x^b, y^b, z^b)$ is centered in the aircraft's Center of Gravity. Its orientation can be observed in Figure 1.

The relation between the body-frame $\mathcal{B}$ and the normal Earth-frame $\mathcal{O}$ is through 3 successive rotations $\phi(t), \theta(t)$ and $\psi(t)$, called Euler angles:

$$R_b^o = R_z(\psi(t))R_y(\theta(t))R_x(\phi(t)) \tag{1}$$

where the subscript b denotes a vector defined in the frame $\mathcal{B}$, which is transformed into a vector in the frame $\mathcal{O}$, denoted with the superscript o.

The kinematic frame $\mathcal{K} = (CG; x^k, y^k, z^k)$ has the origin at the aircraft CG, and the axis x^k points towards the direction of the kinematic speed of the aircraft.

The aerodynamic-frame $\mathcal{A} = (CG; x^a, y^a, z^a)$, with the origin at the aircraft CG, has the x^a axis pointing towards the aircraft's aerodynamic speed. Frame $\mathcal{O}$ is related to $\mathcal{A}$ as:

$$R_a^o = R_z(\chi(t))R_y(\gamma(t))R_x(\mu(t)) \tag{2}$$

Through the angle of attack $\alpha(t)$ and the side-slip angle $\beta(t)$, the relation between $\mathcal{A}$ and $\mathcal{B}$ can be defined as:

$$R_a^b = R_y(-\alpha(t))R_z(\beta(t)) \tag{3}$$

When the aerodynamic velocity $v_a(t) = 0$, the axis of the frame $\mathcal{A}$ and those of the frame $\mathcal{B}$ are aligned.

The relation between the kinematic speed, aerodynamic speed and $V_w(t)$, the velocity of the air mass relative to the ground, namely the wind velocity is given by:

$$V_k(t) = V_a(t) + V_w(t) \tag{4}$$

Assuming zero wind condition, $V_w(t) = 0$, then $V_k(t) = V_a(t)$, namely $\mathcal{A}$ coincides with $\mathcal{K}$.

The angular velocity of $\mathcal{B}$ relative to $\mathcal{O}$ is Ω_{bo}.

Taking into account the symmetry of the aircraft, the inertia matrix is defined in frame $\mathcal{B}$ as:

$$I = \begin{bmatrix} I_x & 0 & -I_{xz} \\ 0 & I_y & 0 \\ -I_{xz} & 0 & I_z \end{bmatrix} \tag{5}$$

3. SYSTEM DESCRIPTION

Figure 1 shows the schematic model of the delta-wing convertible aircraft proposed in this paper. It is a tail-sitter, tilt-body, with two counter-rotating rotors. The wings are symmetric triangular shaped, called delta-wing.

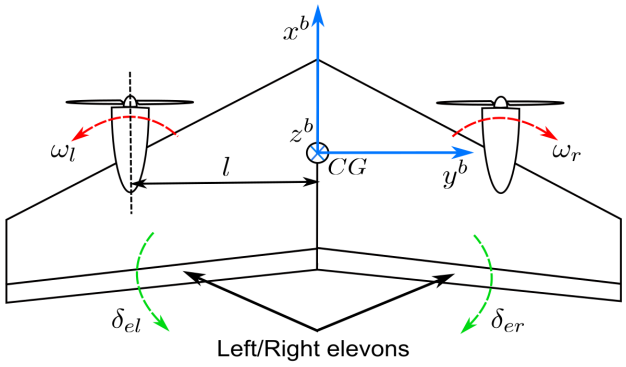

Fig. 1. Schematic model of the convertible aircraft.

Generally, when standard aircraft configurations are considered, the control surfaces include the elevator, the aileron and the rudder (see Beard and McLain (2012)). The aileron, rudder and elevator deflections are denoted respectively as δ_a, δ_r and δ_e.

In the case of a delta-wing configuration, the control surfaces are called elevons. The left and right angular deflections are denoted respectively as δ_{el} and δ_{er}. Driving the elevons differentially $\delta_{el} = -\delta_{er}$ has the same effect as ailerons, providing a torque about the x axis of the aircraft (roll control), instead driving the elevons together $\delta_{el} = \delta_{er}$ has the same effect as an elevator, producing a torque about the y axis of the aircraft (pitch control). The yaw movement is controlled with different spinning of the propellers $\omega_l \neq \omega_r$, called "Differential Propeller

Rotation". Thus, the four control inputs are defined in this way:

- δ_{el}, δ_{er} which are the deflections of the left and right elevons, are expressed in (rad).
- ω_l, ω_r which are the rotation speeds of the left and right counter-rotating propeller-engines, are expressed in (PWM).

When the elevons are deflected downward simultaneously, a nose-up pitching moment is generated, causing the aircraft's nose to pitch up (positive pitch control), instead for upward deflections of the elevons a negative pitch control is generated. When the left elevon is deflected upward and the right elevon is deflected downward, the aircraft rolls to the right (positive roll control), instead for opposite deflections of the elevons a negative roll control is generated.

During the take-off, landing and hover flight modes, the aircraft is positioned vertically on its tail, the aerodynamic velocity is small (or zero during hover) and the thrust from its propellers allows it to take off, hover and land like a helicopter. During the horizontal flight (cruise) the aircraft flies horizontally with higher aerodynamic velocities, like a conventional fixed-wing airplane and the control surfaces become the primary means of maneuvering the aircraft.

4. FORCES AND MOMENTS

4.1 Longitudinal aerodynamics

Lift and drag forces, F_{lift} and F_{drag}, act in the x^b and z^b axis, and the pitch moment, m_{pitch}, in the y^b axis:

$$F_{\text{lift}} = \frac{1}{2}\rho v_a^2 S C_L(\alpha, q, \delta_e) \tag{6}$$

$$F_{\text{drag}} = \frac{1}{2}\rho v_a^2 S C_D(\alpha, q, \delta_e) \tag{7}$$

$$m_{\text{pitch}} = \frac{1}{2}\rho v_a^2 S C_m(\alpha, q, \delta_e) \tag{8}$$

C_L, C_D and C_m are non dimensional aerodynamic coefficients, S (m^2) is the planform area of the wing and ρ is the air density. Phung (2015) proposes to model the lift and drag aerodynamic coefficients as nonlinear functions of α. The lift coefficient is given by the interpolation of two models: one for small angles of attack and one for large angles of attack:

$$\begin{cases} c_{L1}(\alpha, Re) = c_1 \sin(2\alpha) & \text{for } 0 \leq \alpha \leq \alpha_0(Re) \\ & \quad \text{or } 180^o - \alpha_o(Re) \leq \alpha \leq 180^o \\ c_{L2}(\alpha, Re) = c_2 \sin(2\alpha) & \text{otherwise} \end{cases} \tag{9}$$

where Re is the Reynolds number.

A function $\sigma(\alpha, \alpha_o(Re))$, which combines two sigmoid curves is exploited:

$$\sigma(\alpha, \alpha_o(Re)) = \frac{1}{1 + e^{\alpha - \alpha_0(Re)}} + \frac{1}{1 + e^{180° - \alpha - \alpha_0(Re)}} \tag{10}$$

where $\alpha_o(Re)$ represents the stall angle, that depends on the Reynolds number. Thus, the lift, drag and pitch moments are given, respectively, by the following relations. (More details in Beard and McLain (2012)):

$$F_{\text{lift}} = \frac{1}{2}\rho v_a^2 S(c_{L1}(\alpha, Re)\sigma(\alpha, \alpha_o(Re)) \tag{11}$$

$$+ c_{L2}(\alpha, Re)(1 - \sigma(\alpha, \alpha_o(Re))) \tag{12}$$

$$+ C_{L_q}\frac{c}{2v_a}q + C_{L_{\delta_e}}\delta_e) \tag{13}$$

$$F_{\text{drag}} = \frac{1}{2}\rho v_a^2 S(c_1 + 2c_2 \sin^2(\alpha) + C_{D_q}\frac{c}{2v_a}q + C_{D_{\delta_e}}\delta_e) \tag{14}$$

$$m_{\text{pitch}} = \frac{1}{2}\rho v_a^2 S(C_{m_0} + C_{m_\alpha}\alpha + \frac{C_{m_q} c q}{2v_a} + C_{m_{\delta_e}}\delta_e) \tag{15}$$

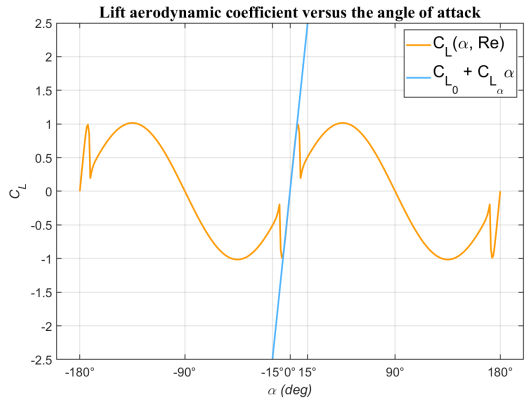

Fig. 2. Lift aerodynamic coefficient C_L versus the angle of attack α, for $Re_{\text{ref}} = 160000$. The linear behaviour $C_L = C_{L_0} + C_{L_\alpha}\alpha$ is maintained for small α.

4.2 Lateral Aerodynamics

The lateral force F_y, the roll moment l and the yaw moment n, are respectively:

$$F_y = \frac{1}{2}\rho v_a^2 S C_Y(\beta, p, r, \delta_{el}, \delta_{er}) \tag{16}$$

$$l = \frac{1}{2}\rho v_a^2 S b C_l(\beta, p, r, \delta_{el}, \delta_{er}) \tag{17}$$

$$n = \frac{1}{2}\rho v_a^2 S b C_n(\beta, p, r, \delta_{el}, \delta_{er}) \tag{18}$$

with b (m) the wingspan of the aircraft, namely the distance from one wingtip to the opposite wingtip, and C_Y, C_L and C_n non dimensional aerodynamic coefficients. Common representations of the aerodynamic coefficients are developed in the following equations and detailed explanations can be found in Beard and McLain (2012):

$$F_y \approx \frac{1}{2}\rho v_a^2 S(C_{Y_0} + C_{Y_\beta}\beta + \frac{C_{Y_p} bp}{2v_a} + \frac{C_{Y_r} br}{2v_a} + C_{Y_{\delta_a}}\delta_a) \tag{19}$$

$$l \approx \frac{1}{2}\rho v_a^2 S b(C_{l_0} + C_{l_\beta}\beta + \frac{C_{l_p} bp}{2v_a} + \frac{C_{l_r} br}{2v_a} + C_{l_{\delta_a}}\delta_a) \tag{20}$$

$$n \approx \frac{1}{2}\rho v_a^2 S b(C_{n_0} + C_{n_\beta}\beta + \frac{C_{n_p} bp}{2v_a} + \frac{C_{n_r} bp}{2v_a} + C_{n_{\delta_a}}\delta_a) \tag{21}$$

4.3 Propulsion Forces and Moments

Based on the Bernoulli's principle, Beard and McLain (2012) proposes the following equations to model the propulsion force and torque in frame $\mathcal{B}$:

$$F_{p_i}^b = \frac{1}{2}\rho S_{\text{prop}} C_{\text{prop}} \left[(k_{\text{motor}}\omega_i)^2 - v_a^2 \;\; 0 \;\; 0\right]^T \tag{22}$$

$$m_t = \left[-K_{T_P}(k_\Omega \omega_i)^2 \;\; 0 \;\; 0\right]^T \tag{23}$$

with $i \in \{l, r\}$. k_{motor} specifies the efficiency of the motor, K_{T_P} is a constant obtained by experiment and $\Omega = (k_\Omega \omega_i)$ the left and right propeller speed.

Each propulsion force induces also a moment, in $\mathcal{B}$, as:

$$m_{p_i} = \overrightarrow{(CG, O_i)}|_{\mathcal{B}} \wedge \left[F_{p_i}^b \;\; 0 \;\; 0\right]^T \tag{24}$$

where $\overrightarrow{(CG, O_i)}|_{\mathcal{B}}$ gives the coordinates of the application point for each of the two propulsion forces in the body-frame, $i \in \{l, r\}$.

Since the two propellers are positioned in a symmetric way in the plane formed by x^b and y^b, with a distance of x_p on the axis x^b and $y_p = \frac{b}{4}$ on y^b, then the total moment from the propulsion forces, in frame $\mathcal{B}$, is:

$$m_p = \left[0 \;\; 0 \;\; y_p(f_{p_l}^b - f_{p_r}^b)\right]^T \tag{25}$$

5. WING-PROPELLER INTERACTION

In order to allow attitude control in hover flight, it is necessary to introduce the slip-stream air induced velocity, due to the spinning of the two propellers:

$$v_i = \frac{1}{2}\left[\sqrt{(v_a\cos(\alpha))^2 + \frac{2F_{\text{thrust}}}{\rho S_{\text{prop}}}} - v_a\cos(\alpha)\right] \tag{26}$$

where S_{prop} (m^2) is the area of the propeller disk. More details in Lustosa et al. (2015). The aerodynamic forces and moments in the slip-stream area are considered to act in the body frame $\mathcal{B}$ and are given by the lift force, the drag force and the pitch moment respectively:

$$L_w = \frac{1}{2}\rho v_i^2 S_w C_{L_{\delta_e}} \delta_e \tag{27}$$

$$D_w = \frac{1}{2}\rho v_i^2 S_w C_{D_{\delta_e}} \delta_e \tag{28}$$

$$m_w = \frac{1}{2}\rho v_i^2 c S_w C_{m_{\delta_e}} \delta_e \tag{29}$$

$S_w \approx \frac{1}{2}S$ is called wet area. It is also considered the roll moment induced by the propeller wing interaction in $\mathcal{B}$:

$$m_e = y_p \frac{1}{2}\rho v_i^2 S_w C_{L_{\delta_a}}(\delta_a) \tag{30}$$

6. TOTAL FORCES AND MOMENTS

The total force vector acting in frame $\mathcal{A}$ is given by:

$$F^a = \begin{bmatrix} X^a(t) \\ Y^a(t) \\ Z^a(t) \end{bmatrix} = F_a^a + R_b^a F_p^b + R_b^a F_w^b \tag{31}$$

with F_a^a defined as the contributions of the lift force, the lateral force and the drag force in frame $\mathcal{A}$:

$$F_a^a = \left[-F_{\text{drag}} \;\; F_y \;\; -F_{\text{lift}}\right]^T \tag{32}$$

and F_w^b as the contribution of the aerodynamic forces due to the wing-propeller interaction:

$$F_w^b = \left[-D_w \;\; 0 \;\; -L_w\right]^T \tag{33}$$

The total torque vector is expressed in frame $\mathcal{B}$:

$$\tau^b = \begin{bmatrix} L^b(t) \\ M^b(t) \\ N^b(t) \end{bmatrix} = \tau_a^b + m_p + m_t + m_w + m_e \tag{34}$$

with the vector τ_a^b defined as follows:

$$\tau_a^b = \begin{bmatrix} L_a^b(t) \\ M_a^b(t) \\ N_a^b(t) \end{bmatrix} = \begin{bmatrix} l \\ m_{\text{pitch}} \\ n \end{bmatrix} \tag{35}$$

7. NONLINEAR DYNAMIC MODEL

The nonlinear model for the convertible aircraft is described using the Newton-Euler formalism, where the equation for the translational motion are expressed in frame $\mathcal{A}$ and those for the rotational motion in frame $\mathcal{B}$:

$$\dot{\xi} = R_a^o V_a^a \tag{36}$$

$$m\frac{dV_a^a}{dt} + \Omega_{ao}^a \wedge mV_a^a = F^a + (R_a^o)^T G^o \tag{37}$$

$$\dot{R}_a^o = R_a^o [\Omega_{ao}^a]_\times \tag{38}$$

$$\frac{d(I\Omega_{bo}^b)}{dt} + \Omega_{bo}^b \wedge I\Omega_{bo}^b = \tau^b \tag{39}$$

$\Omega_{bo}^b = [p, q, r]^T$, where (p, q, r) are the rotational speeds, and $[.]_\times$ represents the skew-symmetric operator. The relation between Ω_{ao}^a and Ω_{bo}^b derives from the following property:

$$\Omega_{ao} = \Omega_{ab} + \Omega_{bo} \tag{40}$$

Projecting this equation in frame $\mathcal{A}$:

$$\Omega_{ao}^a = \Omega_{ab}^a + R_b^a \Omega_{bo}^b \tag{41}$$

and using:

$$\dot{R}_a^b = R_a^b [\Omega_{ab}^a]_\times \quad \Longrightarrow \quad [\Omega_{ab}^a]_\times = (R_a^b)^T \dot{R}_a^b \tag{42}$$

it becomes possible to determine the elements of Ω_{ab}^a as functions of $\alpha(t)$ and $\beta(t)$, and their derivatives:

$$\Omega_{ab}^a = \left[-\dot{\alpha}s\beta \;\; -\dot{\alpha}c\beta \;\; \dot{\beta}\right]^T \tag{43}$$

Substituting (43) in (41), the expression of Ω_{ao}^a as a function of Ω_{bo}^b is obtained.

The complete nonlinear dynamic equations of the model are developed as follows:

$$\dot{x}(t) = c\chi c\gamma v_a \tag{44a}$$

$$\dot{y}(t) = s\chi c\gamma v_a \tag{44b}$$

$$\dot{z}(t) = -s\gamma v_a \tag{44c}$$

$$\dot{v}_a(t) = \frac{X^a}{m} - s\gamma g \tag{44d}$$

$$\dot{\beta}(t) = s\alpha p - c\alpha r + \frac{c\gamma s\mu mg + Y^a}{mv_a} \tag{44e}$$

$$\dot{\alpha}(t) = q - (c\alpha p + s\alpha r)t\beta + \frac{c\gamma c\mu}{c\beta}\frac{g}{v_a} + \frac{Z^a}{c\beta m v_a} \tag{44f}$$

$$\dot{\chi}(t) = \frac{-Z^a s\mu + Y^a c\mu}{v_a mc\mu} \tag{44g}$$

$$\dot{\gamma}(t) = \frac{-c\gamma gm - Y^a s\mu - Z^a c\mu}{v_a m} \tag{44h}$$

$$\dot{\mu}(t) = \frac{-c\mu c\gamma s\beta g}{v_a c\beta} + \frac{pc\alpha + rs\alpha}{c\beta} - \frac{Z^a s\beta}{v_a mc\beta} \tag{44i}$$

$$+ \frac{s\gamma(Y^a c\mu - Z^a s\mu)}{v_a mc\gamma} \tag{44j}$$

$$\dot{p}(t) = \frac{(I_{xz}(I_{xx} - I_{yy} + I_{zz})p}{I_{xx}I_{zz} - I_{xz}^2} - \\ - \frac{(I_{xz}^2 - I_{zz}(I_{yy} - I_{zz}))r)q + I_{xz}N^b + I_{zz}L^b}{I_{xx}I_{zz} - I_{xz}^2} \tag{44k}$$

$$\dot{q}(t) = \frac{-I_{xz}p^2 - r(I_{xx} - I_{zz})p + I_{xz}r^2 + M^b}{I_{yy}} \tag{44l}$$

$$\dot{r}(t) = \frac{((I_{xz}^2 + I_{xx}(I_{xx} - I_{yy}))p}{I_{xx}I_{zz} - I_{xz}^2} - \\ - \frac{I_{xz}(I_{xx} - I_{yy} + I_{zz})r)q + I_{xx}N^b + I_{xz}L^b}{I_{xx}I_{zz} - I_{xz}^2} \tag{44m}$$

8. DIFFERENTIAL FLATNESS ANALYSIS

Flatness is a system property that extends the notion of controllability from linear systems to nonlinear dynamical systems.

In particular, a nonlinear system

$$\dot{x} = f(x, u), \quad u \in \mathbb{R}^m, \quad x \in \mathbb{R}^n, \quad m \leq n \tag{45}$$

is differentially flat if, and only if, there exists an m-dimensional vector

$$y = \phi(x, u, \dot{u}, ..., u^{(\alpha)}) \tag{46}$$

such that x and u can be expressed as functions of the components of y and a finite number of their time derivatives. If one system proves this property is called flat system and the outputs y are called flat-outputs.

Before introducing the overall analysis, it is necessary to remark that the aircraft has to perform a rotation of 90^o around the pitch axis from the vertical take-off to the forward flight, and from the forward flight to the vertical landing. The use of Euler angles $\psi(t)$, $\theta(t)$ and $\phi(t)$ introduces a gimbal lock issue for $\theta(t)$ close to 90^o. Also, the aerodynamic velocity is equal to zero in hover flight and singularity issues can arise. To overcome these problematics, in this paper it is proposed to perform two different flatness analyses: one for the horizontal flight and another one for the vertical take-off, vertical landing and hover flight. More detailed explanations are present in Section 8.1 and Section 8.2.

8.1 Differential flatness analysis for horizontal flight

Assumptions: The equations (44) are considered with the following simplifying assumptions. It is assumed that the side-slip angle β is equal to zero, which implies $Y^a(t) = 0$. Also, the velocity induced by the propeller-wing interaction is assumed to be null and the aerodynamic coefficients are assumed to be linear in $\alpha(t)$.

A set of flat-outputs for this model is given by:

$$y = (x(t), y(t), z(t), \alpha(t)) \tag{47}$$

where $x(t), y(t), z(t)$ is the position of the CG of the aircraft relative to frame $\mathcal{I}$ and $\alpha(t)$ is the angle of attack. The first step consists in deriving from (44a), (44b), (44c), the aerodynamic velocity $v_a(t)$ and the angles $\gamma(t)$ and $\chi(t)$:

$$v_a(t) = \sqrt{\dot{x}^2 + \dot{y}^2 + \dot{z}^2} \tag{48}$$

$$\gamma(t) = \arcsin\left(-\frac{\dot{z}}{v_a}\right) \tag{49}$$

$$\chi(t) = \arctan\left(\frac{\dot{y}}{\dot{x}}\right) \tag{50}$$

Recall that no singularities are present in (49), as in all the following equations, since the aerodynamic velocity is always greater than zero, and it is exploited the atan2 instead of the arctan in (50).

Dividing (44g) by (44h), the angle $\mu(t)$ is obtained:

$$\mu(t) = \arctan\left(\frac{v_a m c(\gamma)\dot{\chi}}{v_a m\dot{\gamma} + c(\gamma)gm}\right) \tag{51}$$

$Z^a(t)$ is computed from (44h):

$$Z^a(t) = -\frac{v_a m\dot{\gamma} + c(\gamma)gm}{c(\mu)} \tag{52}$$

From (44d), $X^a(t)$ is computed:

$$X^a(t) = m\dot{v}_a + s(\gamma)g \tag{53}$$

The pitch angular rate $q(t)$ is obtained from (44f):

$$q(t) = \dot{\alpha} - \frac{c(\gamma)c(\mu)g}{v_a} - \frac{Z^a}{mv_a} \tag{54}$$

Then the roll and yaw angular rates, $p(t)$ and $r(t)$, are obtained from (44j) and (44e) respectively:

$$p(t) = \frac{1}{(1 + \tan^2(\alpha))}\left(\frac{\dot{\mu}}{\cos(\alpha)} - \tan(\alpha)\left(\frac{\cos(\gamma)\sin(\mu)g}{\cos(\alpha)v_a}\right)\right. \tag{55}$$

$$\left. + \frac{Z^a \sin(\mu)\sin(\gamma)}{m\cos(\gamma)v_a\cos(\alpha)}\right) \tag{56}$$

$$r(t) = \frac{v_a \sin(\alpha)p + \cos(\gamma)\sin(\mu)g}{\cos(\alpha)v_a} \tag{57}$$

Finally, the components $L^b(t), M^b(t), N^b(t)$ of the total torque vector τ^b, see (34), are computed from (44k), (44l) and (44m):

$$L^b(t) = I_{xx}\dot{p} - I_{xz}\dot{r} - q((I_{yy} - I_{zz})rI_{xz}p \tag{58}$$

$$M^b(t) = \dot{q}I_{yy} + I_{xz}p^2 + r(I_{xx} - I_{zz})p - I_{xz}r^2 \tag{59}$$

$$N^b(t) = -I_{xz}\dot{p} + I_{zz}\dot{r} - q((I_{xx} - I_{yy})p - I_{xz}r) \tag{60}$$

The total state vector x is now defined as functions of only the flat-outputs and a finite number of their time derivatives, of which the maximum order is four, included in the derivatives of the states: $\dot{v}_a$, $\ddot{v}_a$, $\dot{\gamma}$, $\ddot{\gamma}$, $\dot{\chi}$, $\ddot{\chi}$, $\dot{\mu}$, $\ddot{\mu}$, $\dot{Z}^a$, $\dot{p}$, $\dot{q}$ and $\dot{r}$, which are needed to express all the states found above.

The control inputs can now be derived from τ^b and F^a, since they depend on $L^b(t)$, $M^b(t)$, $N^b(t)$ and $X^a(t)$, $Y^a(t)$ assumed to be equal to zero and $Z^a(t)$, obtained from the flatness analysis.

The following diagram resumes this discussion.

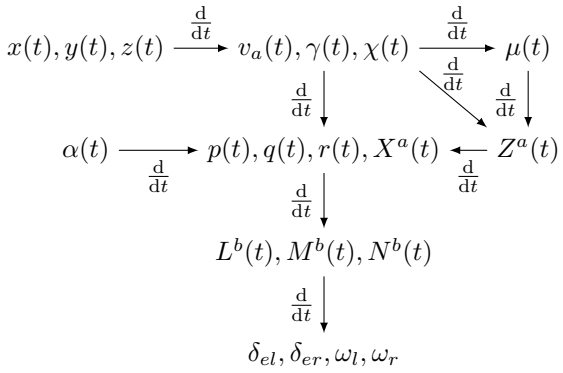

8.2 Differential flatness analysis for vertical take-off, vertical landing and hover flight

The analysis performed in Section 8.1 does not take into account the gimbal lock, introduced in Section 8, and it also raises singularity issues due to the aerodynamic velocity which is zero in hover flight. Therefore another flatness analysis is performed for the vertical take-off/landing and hover flight. In this paper it is proposed to express the equations for the translational motion of the nonlinear dynamic model in frame $\mathcal{I}$ and those for the rotational motion in the body frame $\mathcal{B}$. The orientation of the aircraft from frame $\mathcal{B}$ to frame $\mathcal{O}$, is in terms of vertical Euler angles ϕ_v, θ_v, ψ_v, presented in Castillo et al. (2005), in order to avoid the gimbal lock issue. When the aircraft is in a vertical orientation, the following rotation matrix is used:

$$R^o_{b_v} = R_y\left(\frac{\pi}{2}\right) R_z(\psi_v) R_y(\theta_v) R_x(\phi_v) \tag{61}$$

The resulting model is given by:

$$\dot{\xi} = V^o_o \tag{62}$$

$$m\frac{dV^o_o}{dt} = R^o_b F^b + G^o \tag{63}$$

$$\dot{R}^o_b = R^o_b [\Omega^b_{bo}]_\times \tag{64}$$

$$\frac{d(I\Omega^b_{bo})}{dt} + \Omega^b_{bo} \wedge I\Omega^b_{bo} = \tau^b \tag{65}$$

$V^o_o = [v_{x_o}, v_{y_o}, v_{z_o}]^T$ is the vector of the components of the velocity along the x, y, z directions in the frame $\mathcal{I}$.

Assumptions: Since the aircraft is flying with a null or small aerodynamic speed, then the aerodynamic forces, F_{lift}, F_y and F_{drag}, are neglected. The lift force due to the propeller wing interaction, L_w, is also neglected. Hence:

$$F^b = \begin{bmatrix} F^b_p - D_w & 0 & 0 \end{bmatrix}^T \tag{66}$$

The chosen flat-outputs are:

$$y = (x(t), y(t), z(t), \phi_v(t)) \tag{67}$$

where $x(t), y(t), z(t)$ is the position of the CG of the aircraft relative to frame $\mathcal{I}$ and $\phi_v(t)$ is the roll angle.

From (62) $v_a(t)$ is computed:

$$v_a(t) = \sqrt{\dot{x}^2 + \dot{y}^2 + \dot{z}^2} \tag{68}$$

From (63) $F^b_p - D_w$, $\psi_v(t)$ and $\theta_v(t)$ are obtained:

$$F^b_p - D_w = m\sqrt{\ddot{x}^2 + \ddot{y}^2 + (\ddot{z} - g)^2} \tag{69}$$

$$\psi_v(t) = \arctan\left(\frac{\ddot{y}}{g - \ddot{z}}\right) \tag{70}$$

$$\theta_v(t) = -\arcsin\left(\frac{m\ddot{x}}{F^b}\right) \tag{71}$$

From (64), $p(t)$, $q(t)$ and $r(t)$ are derived:

$$p(t) = -\dot{\psi_v}\mathrm{s}\theta_v + \dot{\phi_v} \tag{72}$$

$$q(t) = \mathrm{s}\phi_v\dot{\psi_v}\mathrm{c}\theta_v + \dot{\theta_v}\mathrm{c}\phi_v \tag{73}$$

$$r(t) = \dot{\psi_v}\mathrm{c}\phi_v\mathrm{c}\theta_v - \dot{\theta_v}\mathrm{s}\phi_v \tag{74}$$

From (65), the components of the total torque vector τ^b are computed:

$$L^b(t) = I_{xx}\dot{p} - I_{xz}\dot{r} - q((I_{yy} - I_{zz})rI_{xz}p) \tag{75}$$

$$M^b(t) = \dot{q}I_{yy} + I_{xz}p^2 + r(I_{xx} - I_{zz})p - I_{xz}r^2 \tag{76}$$

$$N^b(t) = -I_{xz}\dot{p} + I_{zz}\dot{r} - q((I_{xx} - I_{yy})p - I_{xz}r) \tag{77}$$

The control inputs can be now derived from the total torque vector τ^b and the total force vector F^b.

The following diagram resumes this discussion.

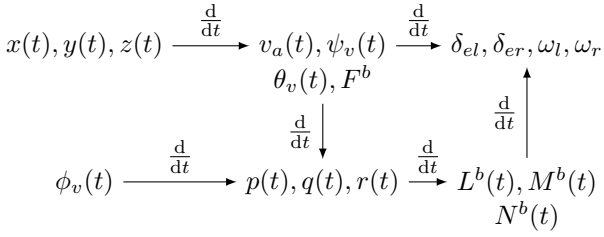

9. CONCLUSIONS

The differential flatness property studied in this paper can be used for the design of feedforward–feedback (FF-FB) control, path planning, and software analytical sensor design in FDI algorithms. In the context of FF-FB control and path planning, an offline pre-recorded trajectory and feedforward control based on the flatness property can be enhanced in real-time by the feedback correction given sensor measurements and observations, in order to obtain fast and precise transitions between the convertible aircraft flight phases (in a similar way to the feedforward flatness based control of a pendulum swing up in Graichen et al. (2007)).

Flat dynamic systems have the inherit property that their inputs and outputs are functions of the flat output and a finite number of its derivatives. This can be used to compute analytical sensor observations, which compared to true sensor outputs, can provide residual signals that can be used for FDI (as described in Rammal et al. (2022)).

REFERENCES

Airimitoaie, T.B., Farges, C., Lavigne, L., and Cazaurang, F. (2019). Convertible delta-wing aircraft for teaching and research. *IFAC-PapersOnLine*, 52(12), 478–483. doi:10.1016/j.ifacol.2019.11.289. Number: 12.

Airimitoaie, T.B., Prieto Aguilar, G., Lavigne, L., Farges, C., and Cazaurang, F. (2018). Convertible aircraft dynamic modelling and flatness analysis. *IFAC-PapersOnLine*, 51(2), 25 – 30. doi:https://doi.org/10.1016/j.ifacol.2018.03.005. 9th Vienna International Conference on Mathematical Modelling.

Basset, P., Tremolet, A., and Lefebvre, T. (2014). Rotary wing uav pre-sizing: past and present methodological approaches at onera. *Aerospace Lab*, 8, 1–12.

Beard, R.W. and McLain, T.W. (2012). *Small Unmanned Aircraft - Theory and Practice*. Princeton University Press.

Castillo, P., Lozano, R., and Dzul, A.E. (2005). *Modelling and control of mini-flying machines*. Springer Verlag London.

Formentin, S. and Lovera, M. (2011). Flatness-based control of a quadrotor helicopter via feedforward linearization. In *IEEE Conference on Decision and Control and European Control Conference*, 6171–6176. IEEE, Orlando, FL, USA. doi:10.1109/CDC.2011.6160828.

Graichen, K., Treuer, M., and Zeitz, M. (2007). Swing-up of the double pendulum on a cart by feedforward and feedback control with experimental validation. *Automatica*, 43(1), 63–71.

Joos, S., Bitzer, M., Karrelmeyer, R., and Graichen, K. (2019). Constrained online trajectory planning for nonlinear flat SISO systems using a switched state variable filter. *Automatica*, 110, 108583. doi:10.1016/j.automatica.2019.108583.

Kaminski, Y.J., Lévine, J., and Ollivier, F. (2018). Intrinsic and apparent singularities in differentially flat systems, and application to global motion planning. *Systems & Control Letters*, 113, 117–124. doi:10.1016/j.sysconle.2018.01.013.

Kubo, D. (2006). Study on design and transitional flight of tail-sitting vtol uav. In *Proceedings of 25th Congress of ICAS*.

Lévine, J. (2009). *Analysis and Control of Nonlinear Systems. A Flatness-based Approach*. Springer-Verlag Berlin Heidelberg.

Louembet, C., Cazaurang, F., and Zolghadri, A. (2010). Motion planning for flat systems using positive B-splines: An LMI approach. *Automatica*, 46(8), 1305–1309. doi:10.1016/j.automatica.2010.05.001.

Lustosa, L.R., Defay, F., and Moschetta, J.M. (2015). Longitudinal study of a tilt-body vehicle: modeling, control and stability analysis. In *2015 International Conference on Unmanned Aircraft Systems (ICUAS)*, 816–824. IEEE.

Lustosa, L.R., Defaÿ, F., and Moschetta, J.M. (2019). Global singularity-free aerodynamic model for algorithmic flight control of tail sitters. *Journal of Guidance, Control, and Dynamics*, 42(2), 303–316.

Lustosa, L.R. (2017). *The Phi-theory approach to flight control design of hybrid vehicles*. Ph.D. thesis, Ph. D. dissertation, Institut Supérieur de l'Aéronautique et de l'Espace ....

Phung, D.K. (2015). *Conception, modeling, and control of a convertible mini-drone*. Theses, Université Pierre et Marie Curie - Paris VI.

Rammal, R., Airimitoaie, T.B., Melchior, P., and Cazaurang, F. (2022). Nonlinear three-tank system fault detection and isolation using differential flatness. *IFAC Journal of Systems and Control*, 21, 100197.

Tal, E. and Karaman, S. (2022). Global incremental flight control for agile maneuvering of a tailsitter flying wing. *Journal of Guidance, Control, and Dynamics*, 45(12), 2332–2349.

Tal, E., Ryou, G., and Karaman, S. (2023). Aerobatic trajectory generation for a vtol fixed-wing aircraft using differential flatness. *IEEE Transactions on Robotics*.

Torres, C.M. (2014). *Fault tolerant control by flatness approach*. Ph.D. thesis, Universidad Autónoma de Nuevo León, Mexico.

WingtraOne (2023). `https://wingtra.com/`. Accessed: 2023-10-23.